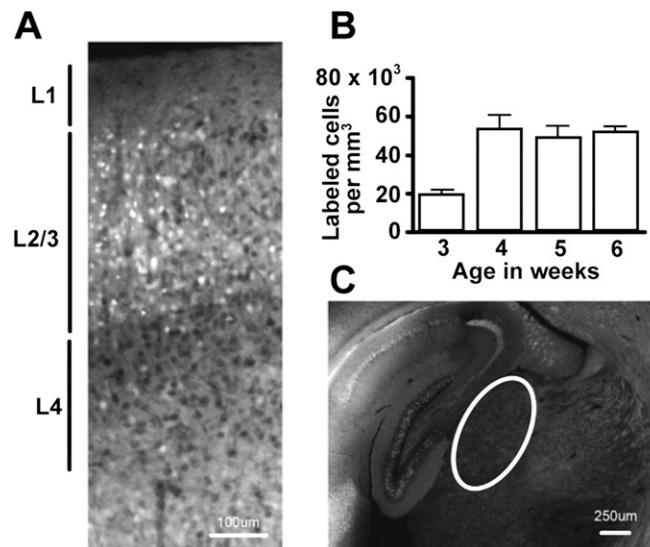


# Supporting Information

Garcia-Junco-Clemente et al. 10.1073/pnas.1309207110



**Fig. S1.** Expression time course of alpha-calcium/calmodulin-dependent kinase II (*CaMK2*–*Cre*) expression in L2/3 of the primary visual cortex. (A) Example of a section taken from the primary visual cortex from a reporter mouse in which *CaMK2*–*Cre* drove the expression of tdTomato (A19 line of mice from Allen Brain Institute; Jackson Laboratories 007909). Note the absence of expression in layer 4. (B) Measures of the number of pyramidal neurons expressing tdTomato in L2/3 in 3-, 4-, 5-, and 6-wk-old mice. Labeling density in adults is consistent with what we previously reported using Zng GFP reporter mice (1). (C) Image of a section through the dorsal lateral geniculate nucleus of the thalamus (delineated by the white oval), which projects to the primary visual cortex. Note the absence of tdTomato expression.

1. Chow DK, et al. (2009) Laminar and compartmental regulation of dendritic growth in mature cortex. *Nat Neurosci* 12(2):116–118.

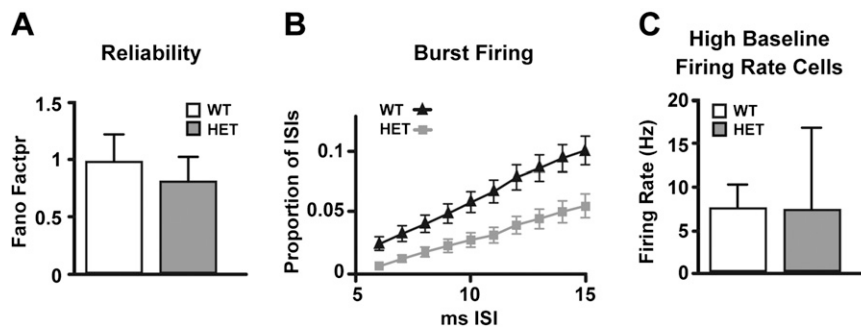


**Fig. S2.** Reliability, burst-firing probability, and visually evoked firing rates of cells with high baseline firing rates. (A) Bar graph showing the mean Fano Factor as a measure for the firing rate reliability for preferred direction visually evoked firing rates of WT and *Pten*<sup>+/-</sup> [heterozygous (HET)] mice. (B) Graph demonstrating the proportion of interspike intervals falling below 5–15 ms in WT and *Pten* HET neurons. Note that *Pten* HET neurons show a higher proportion of low interspike intervals. (C) Mean visually evoked firing rate (baseline subtracted) at the preferred direction for cells with high baseline firing rates (>3 Hz) (presumptive interneurons).

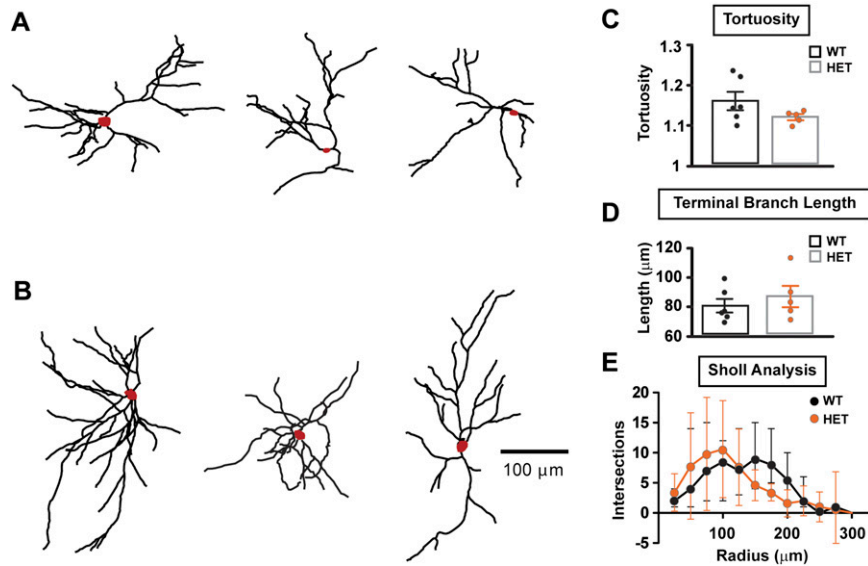


**Fig. S3.** Dendritic morphology of *Pten* HET and control pyramidal neurons. (A and B) NeuroLUCIDA reconstructions (Z projections) of three control and three *Pten* HET neurons filled with Alexa 594 during whole-cell recordings and imaged with a two-photon microscope. Cell bodies are depicted in red. (C and D) Bar graphs demonstrating tortuosity and terminal branch lengths in control (black) and *Pten* HET neurons (orange). (E) Sholl analysis of control (black) and *Pten* HET (orange) neurons, plotting the number of intersections with concentric rings extending from the soma outward. The analysis was performed in the Z projection of the cell. Median and the range for each radius are plotted.

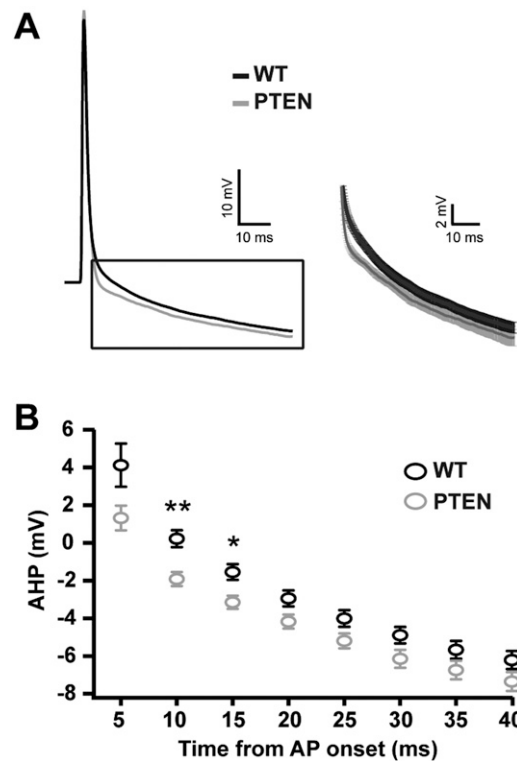


**Fig. S4.** Spike AHPs of *Pten* mutant and control neurons measured in vivo. (A, Left) Average spike waveforms recorded from control and *Pten* mutant neurons. (A, Right) Mean and standard of error values for the spike AHPs shown in the box on the Left. (B) Mean spike AHP amplitudes measured from 5 to 40 ms after spike onset in WT and *Pten* mutant neurons.

**Table S1. Intrinsic properties are altered by *Pten* mutation**

	Control	Control–apamin	Control–paxilline	HET	HET–apamin	HET–paxilline
RMP, mV	$-74.89 \pm 1.13$	$-74.77 \pm 1.55$	$-72.57 \pm 1.5$	$-75.38 \pm 1.04$	$-74 \pm 1.76$	$-75.79 \pm 1.63$
Threshold, mV	$-39.95 \pm 0.47$	$-40.5 \pm 0.68$	$-38 \pm 0.4$	$-41.1 \pm 0.72$	$-38.86 \pm 0.59$	$-41.85 \pm 0.95$
Amplitude, mV	$82.32 \pm 1.71$	$86.4 \pm 1.74$	$90.16 \pm 1.73$	$83.78 \pm 1.86$	$80.2 \pm 2.53$	$89.43 \pm 1.8$
AHP, mV	$11 \pm 0.64^*$	$7.13 \pm 0.58^\dagger$	$11.49 \pm 0.77^\ddagger$	$13.66 \pm 0.59$	$7.51 \pm 0.46$	$15.15 \pm 1.03$
Rise time, ms	$0.3317 \pm 0.0078$	$0.3399 \pm 0.0104$	$0.2815 \pm 0.0044$	$0.3032 \pm 0.0112$	$0.3273 \pm 0.0146$	$0.32 \pm 0.0224$
Width, ms	$1.161 \pm 0.044$	$1.126 \pm 0.037$	$1.2 \pm 0.056$	$1.09 \pm 0.057$	$1.11 \pm 0.072$	$1.378 \pm 0.062$
Memb. const., ms	$18.34 \pm 1.01$	$17.2 \pm 1$	$15.44 \pm 1.23$	$16.39 \pm 0.93$	$18.58 \pm 1.33$	$19.48 \pm 2.65$
Input resistance, M $\Omega$	$220.71 \pm 15.48^\S$	$212.87 \pm 14.5^\S$	$183.74 \pm 13.34^\parallel$	$160.21 \pm 13.59$	$249.34 \pm 26.9$	$146.69 \pm 24.6$
Capacitance, pF	$92.9 \pm 6.28^{**}$	$88.9 \pm 6.72$	$88.99 \pm 9.04$	$115.21 \pm 7.95$	$81.91 \pm 5.49$	$137.5 \pm 19.5$

HET, heterozygous; RMP, resting membrane potential; Memb. const., membrane time constant.

\*AHP, Control vs. HET: paired *t* test; *P* = 0.0045.

<sup>†</sup>AHP, Control–apamin: two-way ANOVA; Bonferroni post-hoc test; *P* < 0.05 for control group; not significant for the apamin group.

<sup>‡</sup>AHP, Control–paxilline: two-way ANOVA; Bonferroni post-hoc test; *P* < 0.05 for control group; *P* < 0.05 for the paxilline group.

<sup>§</sup>Input resistance, Control vs. HET: paired *t* test; *P* = 0.0053.

<sup>§</sup>Input resistance, Control–apamin: two-way ANOVA; Bonferroni post-hoc test; *P* < 0.05 for the control group; not significant for Apamin group.

<sup>||</sup>Input resistance, Control–paxilline: two-way ANOVA; Bonferroni post-hoc test; *P* < 0.05 for the control group; *P* < 0.05 for paxilline group.

\*\*Capacitance, Control vs. HET: paired *t* test; *P* = 0.0079.